Temperature-Insensitive and Two-Sided Endless Polarization Control

Benjamin Koch, Reinhold Noé, *Senior Member, IEEE*, Vitali Mirvoda, and David Sandel, *Member, IEEE*

***Abstract*— Endless input polarization tracking is demonstrated at 60 krad/s over a temperature ramp from 0 °C to 60 °C and at 15 krad/s with simultaneous endless variations at 200 rad/s of the analyzed output polarization.**

***Index Terms*— Optical fiber communication, optical fiber polarization, quadrature phase shift keying.**

I. Introduction

ENDLESS optical polarization control is a key enabler for benefitting from polarization multiplex in transmission systems with direct detection [1]–[3]. Using optical polarization demultiplex, PDM-DQPSK receivers save power and cost compared to coherent receivers. In this case, the polarization controller transforms the variable input polarization of a channel into a fixed eigenstate of a polarization beam splitter. The outputs of the splitters deliver the two separated polarization channel signals. Feedback for the controller is provided by analyzing cross channel interference [3], [4]. For the 200 Gb/s experiment [3], PMF was used between controller and beam splitter to fix the output polarization of the controller. This allowed the use of a single Soleil-Babinet compensator (SBC) with a maximum retardation of π for control [5]. One-sided polarization control has become very fast, reaching 100 krad/s [6] or even 140 krad/s [7].

When working with SMF at the output (without PMF), be it for cost or coupler size or other practical reasons, both input and output polarization changes have to be tracked simultaneously. Addressing this scenario we have enhanced our polarization algorithm for two-sided control. The modified system is capable of tracking polarization changes caused by manual fiber handling at the output side, while maintaining krad/s-tracking speed at the input side. We also show, for the first time, that control is stable while the ambient temperature follows a ramp from 0 °C to +60 °C.

Manuscript received July 26, 2012; revised September 17, 2012; accepted September 17, 2012. Date of publication September 19, 2012; date of current version October 31, 2012.

B. Koch and R. Noé are with the University of Paderborn, Paderborn 33098, Germany, and also with Novoptel GmbH, EIM-E, Paderborn 33098, Germany (e-mail: koch@ont.upb.de; noe@upb.de).

V. Mirvoda and D. Sandel are with the University of Paderborn, Paderborn 33098, Germany (e-mail: mirvoda@ont.upb.de; sandel@ont.upb.de).

Color versions of one or more of the figures in this letter are available online at http://ieeexplore.ieee.org.

Digital Object Identifier 10.1109/LPT.2012.2219857

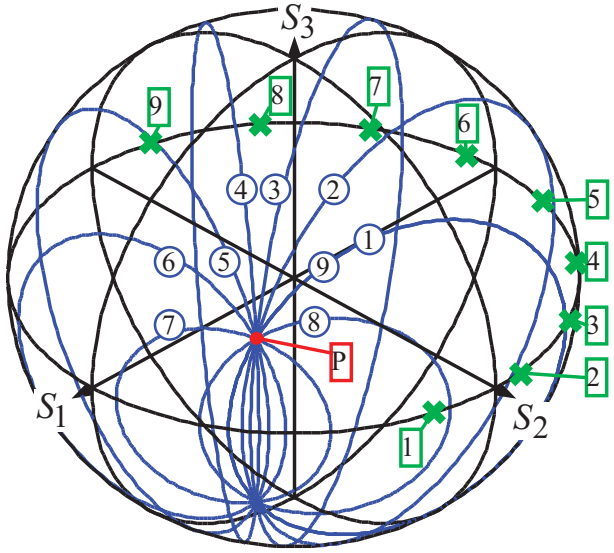

Fig. 1. Only when input polarization reaches sought output polarization (red dot P on Poincaré sphere) does the retardation of the Soleil-Babinet compensator reach 2π. To prevent overflow, SBC eigenmodes (green x) are then reoriented to the opposite position (from positions 1 to 9). Corresponding polarization transformations (blue circles, with encircled numbers 1 to 9) are full circles around eigenmode axes. All these circles start and end at point P. Circles 1 and 9 are identical except for the rotation sense. Retardation overflow is thereby prevented, or by more tentative eigenmode orientation changes.

II. Control Principle

A single SBC can transform any input polarization into any output polarization [8]. Only orientation and retardation have to be varied by a gradient search on an error signal. This is normal control which is executed at almost all times. The SBC orientation can vary arbitrarily but the retardation will stay between 0 and 2π. Only if input and output polarizations happen to become identical the retardation can reach the value 2π, i.e. its permitted maximum. Overflow must now be prevented. Upon detection of this status and retardation value, by analysis of $LiNbO_3$ electrode voltages, the SBC orientation is changed to opposite, at constant retardation of 2π. The reorientation must be completed while the two polarizations, denoted by the red dot P on the Poincaré sphere (Fig. 1) remain identical. During this process the linear SBC eigenmodes subsequently assume various positions 1 to 9, denoted by green x on the equator. The corresponding polarization transformations, all of them with 2π of retardation, are full

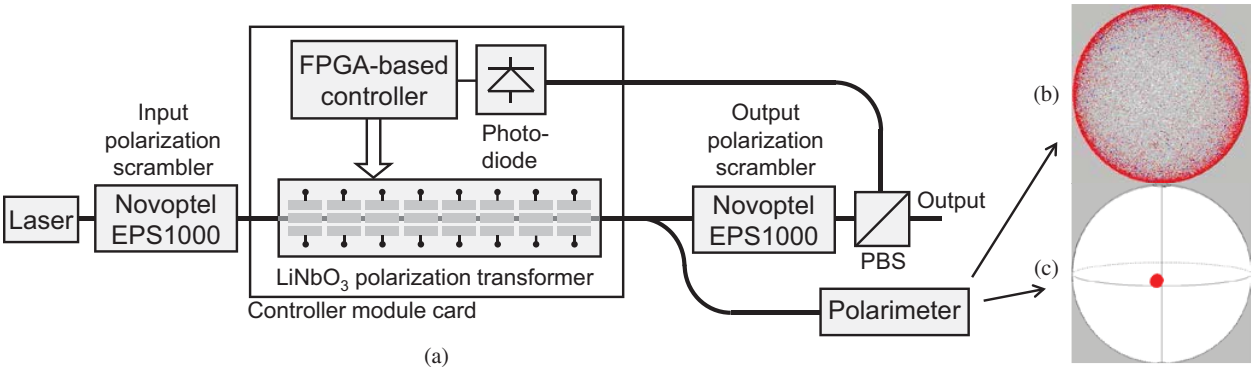

Fig. 2. (a) Two-sided polarization control using two endless polarization scramblers. Polarimeter screenshot (b) without polarization control and (c) after 10 minutes with 60 krad/s input scrambling and output scrambler halted.

circles, drawn in blue and also marked by encircled numbers 1 to 9. Each of these transforms the input polarization into the output polarization, which coincides with the former. Circles 1 and 9 are identical, except that they turn with opposite senses, because they originate from eigenmodes 1 and 9, which are orthogonal polarizations. If input and output polarizations continue changing in the same directions as before, when they approached the retardation limit 2π, then the controller will subsequently be able reduce the retardation below 2π, rather than being forced to increase it. Retardation overflow is thereby prevented. If polarizations change during or after eigenmode reorientation in other directions then the eigenmodes have to be reoriented again until it is indeed possible to decrease retardation.

III. Setup

Fig. 2(a) shows the setup for two-sided endless polarization control. A 10 Mrad/s endless polarization scrambler (Novoptel EPS1000) is placed behind an unmodulated laser source. The scrambler is configured as a rotatable halfwave plate (HWP) between two trios of rotatable quarterwave plates (QWPs). The HWP rotates at high speed, generating circles on the Poincaré sphere. The QWPs rotate at lower, incommensurate rates in order to change sizes and orientations of the circles. At 60 krad/s scrambling rate the scrambler output polarizations are spread randomly over the whole Poincaré sphere [see Fig. 2(b)].

The polarization controller transforms the scrambled input polarization into an eigenstate of the polarization beam splitter (PBS), while the polarization transformations of a second polarization scrambler placed just before the PBS are additionally compensated. All this is done by minimizing the optical power at one of the PBS outputs, while the other output carries the re-polarized signal.

Our realized two-sided endless polarization controller is functionally equivalent to the principle described in Section II. However, for ease of implementation, eight SBCs with smaller retardations are made to work similarly to the single one with 2π retardation. A commercial $LiNbO_3$ polarization transformer with X cut and Z propagation is used for this purpose. Electrode structure is shown in Fig. 2(a), driving and calibration are detailed in [9]. The difference with respect

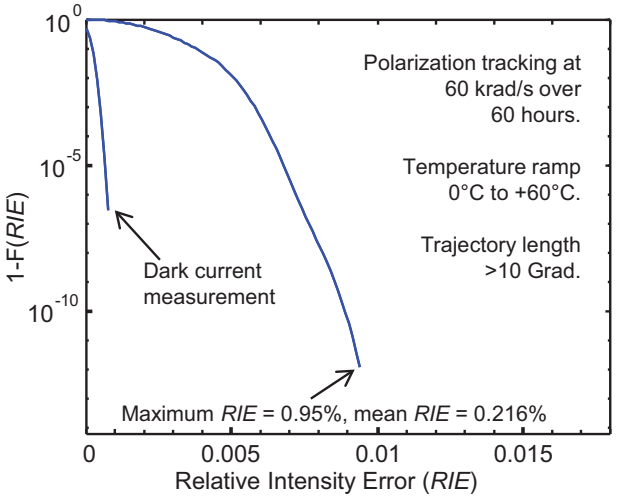

Fig. 3. Complementary cumulative distribution function 1−F(*RIE*) of relative intensity error at 60 krad/s input polarization scrambling and 60 °C temperature changes over 60 h.

to our earlier experiments [3], [7], [9], [10], where only a single polarization was tracked endlessly, is that the overall SBC retardation is limited to a maximum of 2π, not just π. SBC reorientation prevents total retardation from an overflow beyond 2π and subsequently leads to a retardation decrease.

IV. Experimental Results

At first, the output polarization scrambler is halted. Under control, the output polarization of the controller is constant while all input polarization changes are compensated. Fig. 2(c) shows a screenshot of the polarimeter after 10 minutes of 60 krad/s input polarization scrambling. The accumulated polarization states form a nicely confined spot, indicating accurate polarization control. The spot radius is about 0.08 rad.

Next, the whole polarization controller module card is placed in a climate chamber. During a measurement time of 60 hours, the temperature in the chamber is increased from initially 0 °C to finally +60 °C. In order to get an accurate measure of all polarization errors during the measurement time, samples of the relative intensity error (*RIE*) are accumulated into a histogram, roughly every 140 ns. Fig. 3 shows the complementary cumulative distribution function of the *RIE*,

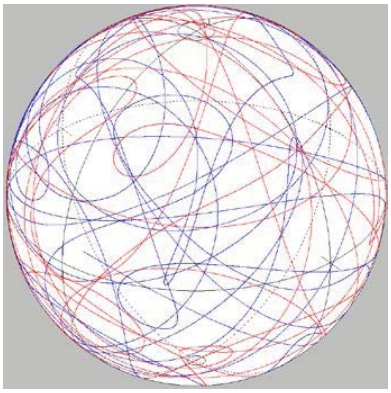

Fig. 4. Polarimeter screenshot during tracking of 15 krad/s input polarization changes and additional 5 rad/s output polarization changes.

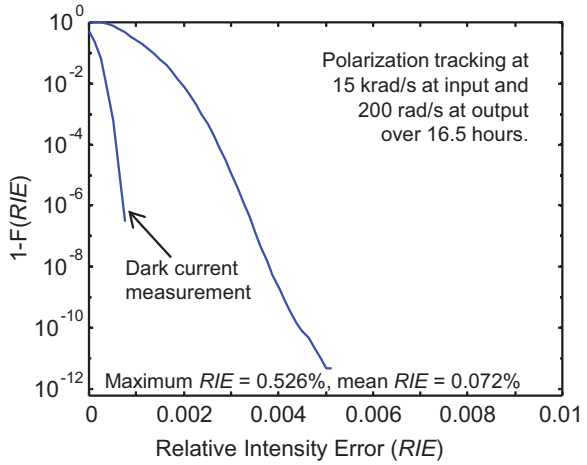

Fig. 5. Complementary cumulative distribution function 1−F(*RIE*) of relative intensity error at 15 krad/s input polarization scrambling and 200 rad/s output polarization scrambling over 16.5 h.

which represents the probability that a given *RIE* is surpassed. The maximum *RIE* of 0.95% corresponds to a polarization error of 0.195 rad. Mean *RIE* and polarization error were 0.216% and 0.093 rad, respectively. Note that parts of the measured mean error are caused by a temperature-induced drift of the point of $RIE = 0$ which is determined by a short measurement only before the experiment (left curve).

Compared to earlier experiments with temperature changes [10], the tracking speed is now significantly higher. The present experiment includes temperature changes of the whole board, not just of the $LiNbO_3$ element. Furthermore, not only specific temperatures but a whole temperature range is covered by uninterrupted tracking during a continuous temperature ramp.

Back at room temperature and with input polarization scrambling at 15 krad/s, the output polarization scrambler is switched on. At output scrambling speeds of up to 5 rad/s, the output polarization changes are accurately tracked by the polarimeter. Fig. 4 show the output polarization trajectory, which follows and compensates the transformations of the output polarization scrambler. The shown trajectory is clean and solid, without glitches. This indicates accurate tracking of both input and output polarization.

Finally the output scrambler is set to a scrambling speed of 200 rad/s, which is in the same order of magnitude as the fastest expected polarization changes caused by manual fiber handling. For accurate error measurement, another histogram is recorded during a measurement time of 16.5 hours. The complementary cumulative distribution function is shown in Fig. 5. Mean and maximum *RIE*s are 0.072% and 0.526%, respectively (right curve). Corresponding mean and maximum polarization errors are just 0.054 rad and 0.145 rad, respectively. This control quality easily suffices even for demanding applications.

V. Conclusion

We have demonstrated, for the first time, endless polarization control at krad/s speed over an ambient temperature ramp from 0 °C to 60 °C. At polarization changes of up to 60 krad/s, a polarization trajectory of >10 Gigarad length was thereby tracked during 60 hours. Mean and maximum polarization errors were of 0.093 rad and 0.195 rad, respectively.

Our simultaneous tracking of 15 krad/s input and 200 rad/s output polarization changes has demonstrated two-sided endless polarization control, for the first time with multi-krad/s tracking speed (at one side). Tracked trajectory length in a 16.5-hour measurement was 700 Mrad. Mean and maximum polarization errors were only 0.054 rad and 0.145 rad, respectively.

Two-sided polarization control makes automatic polarization demultiplexers much more versatile and cheaper because no PMF is needed between polarization transformer and beam splitter or receiver. Furthermore, this allows the polarization tracking of single- or dual-polarization signals with user-supplied error signals.

References

[1] S. Yunfeng, *et al.*, "Design of polarization de-multiplexer and PMD compensator for 112 Gb/s direct-detect PDM RZ-DQPSK systems," *J. Lightw. Technol.*, vol. 28, no. 22, pp. 3282–3293, Nov. 15, 2010.

[2] J. Zhang, *et al.*, "Transmission of 112 Gb/s PM-RZ-DQPSK over 960 km with adaptive polarization tracking based on power difference," in *Proc. ECOC 2010*, pp. 1–2, paper P2.09.

[3] B. Koch, R. Noé, V. Mirvoda, D. Sandel, V. Filsinger, and K. Puntsri, "40-krad/s polarization tracking in 200-Gb/s PDM-RZ-DQPSK transmission over 430 km," *IEEE Photon. Technol. Lett.*, vol. 22, no. 9, pp. 613–615, May 1, 2010.

[4] S. Bhandare, *et al.*, "5.94-Tb/s 1.49-b/s/Hz (40×2×2×40 Gb/s) RZ-DQPSK polarization-division multiplex C-band transmission over 324 km," *IEEE Photon. Technol. Lett.*, vol. 17, no. 4, pp. 914–916, Apr. 2005.

[5] R. Noé, *et al.*, "Endless polarization control systems for coherent optics," *J. Lightw. Technol.*, vol. 6, no. 7, pp. 1199–1207, Jul. 1988.

[6] *Commercial Polarization Control Up to 100 krad/s*. (2012, Jun. 25) [Online]. Available: http://www.novoptel.de/Control/Control_EPC1000_en.php

[7] B. Koch, *et al.*, "140 krad/s, 254-Gigaradian endless optical polarization tracking, independent of analyzed output polarization," in *Proc. OFC 2012*, pp. 1–3, paper OTu1G.

[8] N. G. Walker and G. R. Walker, "Polarization control for coherent communications, *J. Lightw. Technol.*, vol. 8, no. 3, pp. 438–458, Mar. 1990.

[9] A. Hidayat, *et al.*, "High-speed endless optical polarization stabilization using calibrated waveplates and field-programmable gate array-based digital controller," *Opt. Express*, vol. 16, no. 23, pp. 18984–18991, 2008.

[10] B. Koch, *et al.*, "Robust, wavelength- and temperature-insensitive 14 krad/s endless polarization tracking over 2.5 Grad," in *Proc. OFC/NFOEC 2009*, San Diego, CA, Mar., pp. 1–3, paper JThA63.